J Mater Sci: Mater Med (2007) 18:1211–1218
DOI 10.1007/s10856-007-0157-7

Osteoprogenitor response to low-adhesion nanotopographies originally fabricated by electron beam lithography

Andrew Hart · Nikolaj Gadegaard · Chris D. W. Wilkinson · Richard O. C. Oreffo · Matthew J. Dalby

Received: 20 May 2005 / Accepted: 23 March 2006 / Published online: 3 February 2007

Abstract It is considered that cells can use filopodia, or microspikes, to locate sites suitable for adhesion. This has been investigated using a number of mature cell types, but, to our knowledge, not progenitor cells. Chemical and topographical cues on the underlying substrate are a useful tool for producing defined features for cells to respond to. In this study, arrays of nanopits with different symmetries (square or hexagonal arrays with 120 nm diameters, 300 nm center–centre spacings) and osteoprogenitor cells were considered. The pits were fabricated by ultra-high precision electron-beam lithography and then reproduced in polycarbonate by injection moulding with a nickel stamp. Using scanning electron and fluorescence microscopies, the initial interactions of the cells via filopodia have been observed, as have subsequent adhesion and cytoskeletal formation. The results showed increased filopodia interaction with the surrounding nanoarchitecture leading to a decrease in cell spreading, focal adhesion formation and cytoskeletal organisation.

A. Hart · M. J. Dalby (✉)
Centre for Cell Engineering, Division of Infection and Immunity, Institute of Biomedical and Life Sciences, Joseph Black Building, University of Glasgow, Glasgow G12 8QQ, UK
e-mail: m.dalby@bio.gla.ac.uk

N. Gadegaard · C. D. W.Wilkinson
Centre for Cell Engineering, Department of Electronics and Electrical Engineering, Rankine Building, University of Glasgow, Glasgow G12 8QQ, UK

R. O. C.Oreffo
Bone and Joint Research Group, DOHAD, University of Southampton, Southampton S016 6YD, UK

1 Introduction

It has been known for many years that cells will react to the shape of their environment [1]. Considerable research effort has been directed at elucidating the range of cell responses to microtopography and, to date, every cell type examined (including platelets which lack a nucleus) have been shown to respond to their surrounding topography [2–7]. Examples of cell response include changes in adhesion, cytoskeletal organisation, motility and migration, contact guidance, macrophage activation and differential gene expression.

The properties of the materials that form the underlying surface can be expected to change the material/protein interactions that are critical to subsequent cell adhesion and response. It is through protein absorption that a cell will be able to/unable to form focal adhesions [8, 9]. The formation of adhesions is critical for all other cell response as the cytoskeleton is anchored to the adhesion sites and cytoskeletal organisation is critical for cellular signalling events leading to proliferation and differentiation [10, 11] (and so the embryology of the tissue). Failure of cell adhesion will, ultimately, result in cell death (apoptosis).

In the process of cell adhesion, it is proposed that cells 'probe' the material surface with filopodia, or microspikes [12]. Filopodia are actin driven structures that the cell can move in a sweeping motion at the cell's leading edge. Recent evidence has shown that as a cell finds a suitable anchorage site, vinculin expression is observed at the tip of the filopodia—the start point of focal adhesion formation—and that the

filopodia may guide the cells lamellipodia (ruffled leading edge) to the sight of preferential adhesion [12, 13].

The use of osteoblast and fibroblast culture models indicate that such sights of preferential adhesion may be mainly chemical or they may be purely topographical. Examples of the former include the chemical islands of HAPEX^{TM} [14], where hydroxyapatite is presented to cells dispersed in a polyethylene matrix—note that the matrix may be varied to e.g. polymethylmethacrylate [15] or the bioactive component may be varied to e.g. Bioglass® [16] and the effects remain) or topographical, e.g. grooves, pillars, islands etc [12, 13, 17, 18]. Topography presents an ideal system to study filopodial interaction as the placing and size of features can be controlled with nanometer precision, using patterns generated by electron beam lithography.

Electron beam lithography (e-beam) is a development of the microelectronic industry's drive for miniturization. E-beam allows down to 5 nm resolution in the *X* and *Y* planes [19, 20]. Patterns are produced by exposing a radiation sensitive resist to electron beams (analogous to photography). This makes the resist resistant/not-resistant to development (depending whether a positive or negative resist is used). Once developed, dry (ion) etch can be used to sculpt structures into the bulk material (e.g. silicon for the production of microelectronics) [21].

Subsequent to this, a system of nickel sputtering followed by electroplating and fall away of the master silicon substrate allows the fabrication on nickel (Ni) shims. These are negative copies of the master material. Hot polymers can then be embossed/injection moulded against the shims giving reproductions of the masters with down to 5 nm resolution when optimised [22]. These methods of mechanical transfer allow the rapid and cheap production of the quantity of samples required for biological evaluation.

Human mesenchymal stromal cells (HMSC's, osteoprogenitor cells) derived from bone marrow have been used in this study of filopodia interaction with surrounding nanoarchitecture, specifically, 120 nm diameter e-beam pits with square (sq) and hexagonal (hex) symmetry injection moulded against shims into polycarbonate (PC). Scanning electron microscopy (SEM) and fluorescent microscopy have been used to quantify filopodia production and pit interaction. Fluorescent observation of focal adhesion formation and cytoskeletal organisation have also been made.

2 Methods

2.1 Nano patterning and die fabrication

Samples were made in a three-step process of electron beam lithography, nickel die fabrication and injection moulding. Silicon substrates were coated with ZEP 520A (Zeon corporation) resist to a thickness of 100 nm. Samples were baked for a 1–2 h at 180 °C prior to exposure in a Leica LBPG 5-HR100 beamwriter at 50 kV. An 80 nm spot size was used, resulting in pits with 120 nm diameters. The pitch between the pits was 300 nm. Both hexagonal and square pit arrangements were used. After exposure the samples were developed in *o*-xylene at 23 °C for 60 s and rinsed in copious amounts of 2-propanol before being blown dry with filtered nitrogen. For more information about the procedure see ref. [21].

Nickel dies were made directly from the patterned resist samples. A thin (50 nm) layer of Ni–V was sputter coated on the samples. That layer acted as an electrode in the subsequent electroplating process. The dies were plated to a thickness of ca. 300 μm. For more information about the procedure see ref. [22].

Polymeric replicas were made in poly(carbonate), PC, by injection moulding. We have used DVD grade PC (Macrolon DP1-1265, Bayer) as it is known to have very good replication capabilities [23]. Further details are given in ref. [22].

2.2 Cell isolation

2.2.1 Human bone marrow cells (HMSC)

Bone marrow samples (female, $n = 4$; mean 76 ± 8 years of age) were obtained from hematologically normal patients undergoing routine hip replacement surgery. Only tissue that would have been discarded was used with the approval of the Southampton & South West Hants Local Research Ethics Committee. Primary cultures of bone marrow cells were established as previously described [24, 25].

Marrow aspirates were washed in α-MEM, then the suspended cells were centrifuged at 250×*g* for 4 min at room temperature. The cell pellet was resuspended and plated to culture flasks at appropriate densities with non-adherent cells and red blood cells were removed via a PBS wash and media change after 1 week. Cultures were maintained in basal media (α-MEM containing 10% FCS) at 37 °C, supplemented with 5% CO_2. All studies were conducted using passage 1 and passage 2 cells.

2.3 Cell culture

HBMC were seeded onto the test materials at a density of 1×10^4 cells per sample in 1 ml of complete medium. The medium used was αMEM with 10% FCS (Life Technologies, UK). The cells were incubated at 37 °C with a 5% CO_2 atmosphere, and the medium was changed twice a week.

2.4 Image analysis of cell perimeter and area

After 4 days of culture, the cells on the test materials were fixed in 4% formaldehyde/PBS at 37 °C for 15 min. The cells were then stained for 2 min in 0.5% Coomasie blue in a methanol/acetic acid aqueous solution, and washed with water to remove excess dye. Samples could then be observed by light microscopy and automated detection of cell outline was used to calculate individual cell perimeters. The image analysis software was downloaded from the National Institute of Health (USA) (Image J, http://rsb.info.nih.gov/ij/).

2.5 Scanning electron microscopy of cell filopodia

The cells were fixed with 1% gluteraldehyde (Sigma, UK) buffered in 0.1 M sodium cacodylate (Agar, UK) (4 °C, 1 h) after a 4 day incubation period to allow the viewing of individual cells. The cells were then post-fixed in 1% osmium tetroxide (Agar, UK) and 1% tannic acid (Agar, UK) was used as a mordant, then dehydrated through a series of alcohol concentrations (20, 30, 40, 50, 60, and 70%), stained in 0.5% uranyl acetate, followed by further dehydration (90, 96, and 100% alcohol). The final dehydration was in hexamethyl-disilazane (Sigma, UK), followed by air-drying. Once dry, the samples were sputter coated with gold before examination with either a Hitachi S800 or S4700 field emission SEM (both used at an accelerating voltage of 10 keV).

2.6 Fluorescent staining

After 4 days of culture the cells on the test materials were fixed in 4% formaldehyde/PBS, with 1% sucrose at 37 °C for 15 min, to allow the viewing of individual cells. When fixed, the samples were washed with PBS, and a permeabilising buffer (10.3 g sucrose, 0.292 g NaCl, 0.06 g $MgCl_2 \cdot 6H_2O$, 0.476 g Hepes buffer, 0.5 ml Triton X, in 100 ml water, pH 7.2) added at 4 °C for 5 min. The samples were then incubated at 37 °C for 5 min in 1% BSA/PBS. This was followed by the addition of an anti-vinculin primary antibody (1:100 in 1% BSA/PBS Hvin1 monoclonal anti-human raised in mouse (IgG1), Sigma, Poole, UK) for 1 h (37 °C). Simultaneously, rhodamine conjugated phalloidin was added for the duration of this incubation (1:100 in 1% BSA/PBS, Molecular Probes, Oregon, USA). The samples were next washed in 0.5% Tween 20/PBS (5 min × 3). A secondary, biotin conjugated antibody, (1:50 in 1% BSA/PBS, monoclonal horse anti-mouse (IgG), Vector Laboratories, UK) was added for 1 h (37 °C) followed by washing. A FITC conjugated streptavidin third layer was added (1:50 in 1% BSA/PBS, Vector Laboratories, UK) at 4 °C for 30 min, and given a final wash. Samples were then viewed by fluorescence microscopy (Zeiss Axiovert 200M).

2.7 Statistics

Student's *t*-test (for two samples, assuming unequal variances) was used to compare statistical significances. Results of $p < 0.05$ were considered significant (differences of $p < 0.05$ denoted by *, differences of $p < 0.01$ denoted by **).

3 Results

Using e-beam fabrication and Ni intermediaries, embossed replicas of the original master substrates have been produced with good fidelity in PC. The imprints comprised 120 nm diameter pits with 300 nm centre to centre spacing in square (sq) and hexagonal (hex) arrangements (Fig. 1).

Measurement of perimeter showed the cells on the test materials to be less well spread than those cultured on planar control samples (Fig. 2A). Measurement of filopidia per cell showed no differences (Fig. 2B). However, normalization of filopodia counts by dividing the mean numbers of filopodia by measured cell perimeters has shown increased numbers of filopodia being produced per μm of membrane in cells on the nanomaterials compared to cells on planar controls (Fig. 2). Using high-resolution SEM, allowed the further calculation of percentage filopodia/pit interaction defined by the tip of a filopodia contacting the lip, or centre, of a pit (Figs. 3, 4). It was found that there was an average of 67% filopodial/pit interaction on the square structures and 66% interaction on the hexagonal structures (noting that no filopodia/feature interaction could not be calculated for the control samples as they have no features).

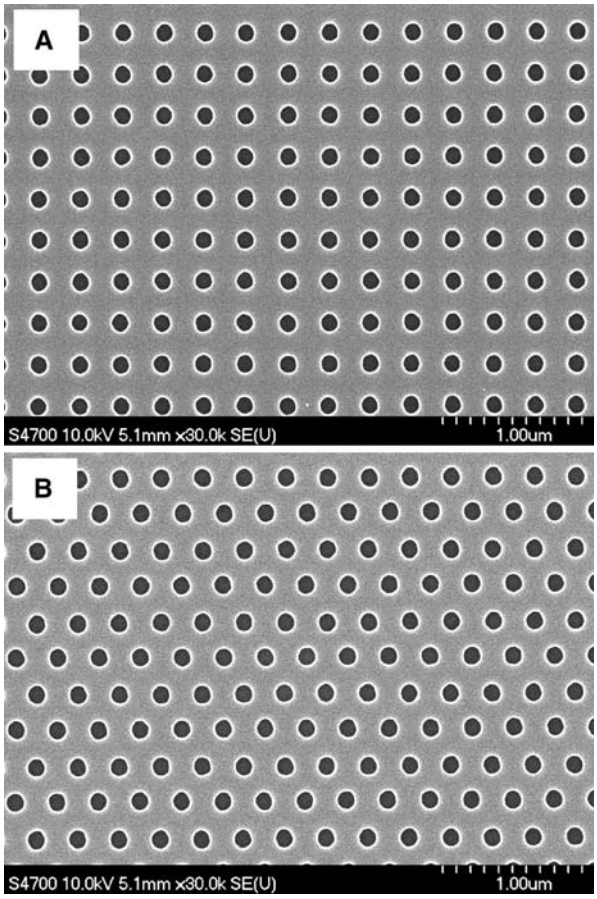

Fig. 1 Scanning electron micrographs of nanopitted surfaces with 120 nm diameter pits with 300 nm centre-centre spacing with (**A**) square (sq) and (**B**) hexagonal (hex) arrangements

Area measurements (Fig. 2D) confirmed perimeter results and showed that the cells were significantly less spread ($p < 0.05$) on the sq topography. This became even more significant ($p < 0.01$) for osteoprogenitor cells cultured on the hex topography.

Observation of vinculin in focal adhesions showed that culture of the progenitor cells on the nanotopographies reduced the cells ability to form focal adhesions (Fig. 5). Cells cultured on sq had visible adhesions, but fewer in number and less clear (Fig. 5B). Cells cultured on hex had very few notable adhesions (Fig. 5C).

Fluorescent staining of actin showed that whilst cells cultured on the planar control material had many stress fibres throughout the cytoplasm, cells cultured on both the square and hexagonal pits had mainly cortical actin and many filopodia (Fig. 6). The morphology of the cells, revealed by actin staining, also showed the cells on the low-adhesion structured to be more stellate than cells cultured on planar control.

4 Discussion

Nanoscale pits have previously been shown to have low-adhesion properties to epitinon fibroblasts [26, 27] and to dermal fibroblasts [13, 28]. With the HMSC's, cells were seen to adhere, but to be less well spread with stellate morphology and smaller perimeters and areas when cultured on the nanopits compared to cells

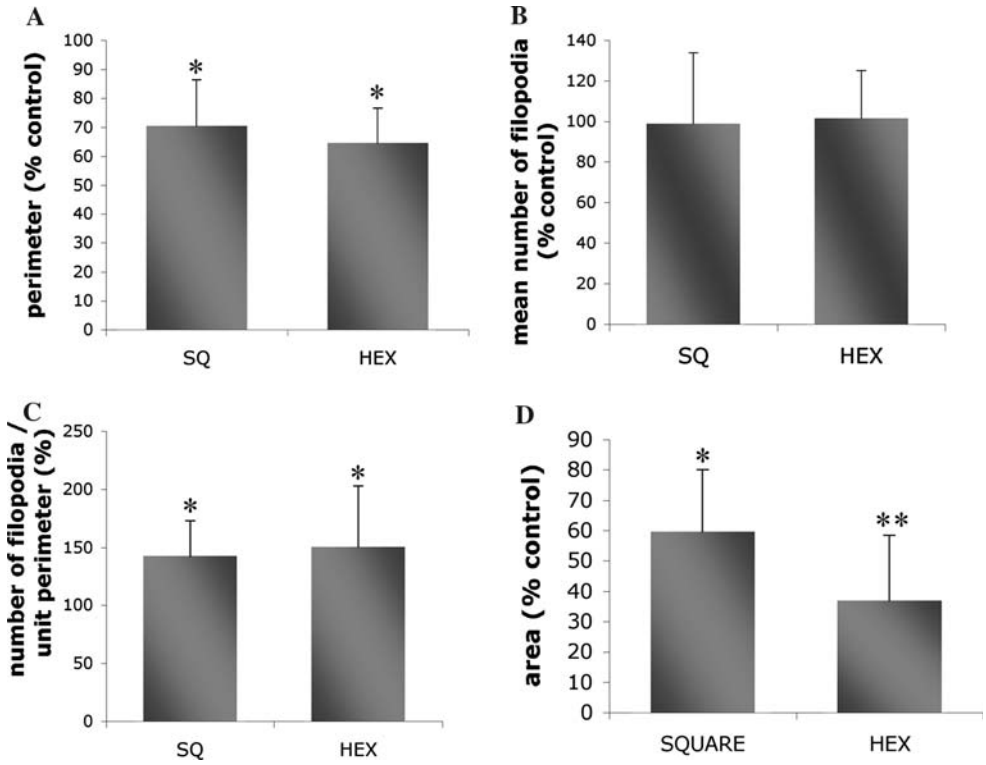

Fig. 2 Graph showing (**A**) mean perimeter, (**B**) mean number of filopodia, (**C**) mean number of filopodia/ perimeter and (**D**) mean area as percentage of control (cells on planar material) for cells cultured on square (sq) and hexagonal (hex) materials. Results are mean percentage of control, * = *t*-test $p < 0.05$ compared to control, ** = *t*-test $p < 0.01$ compared to control

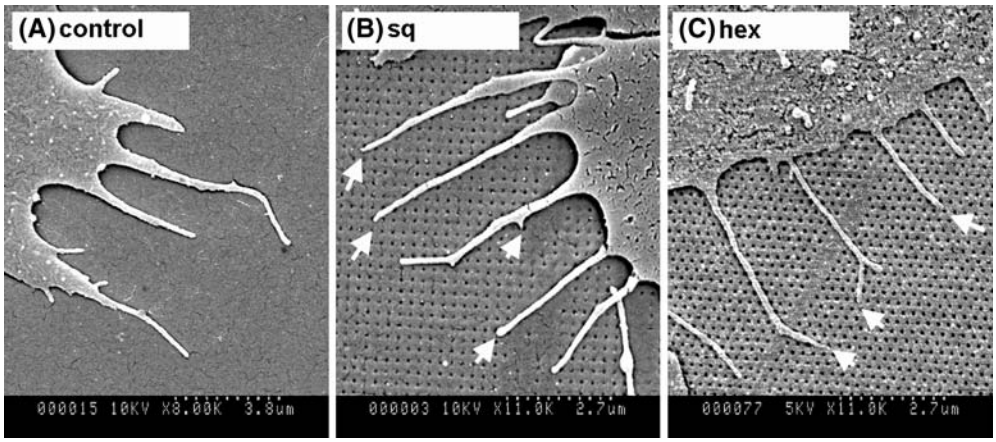

Fig. 3 Scanning electron micrographs of osteoprogenitor cell filopodia cultured on (**A**) planar control, (**B**) square (sq) nanopit arrays and (**C**) hexagonal (hex) nanopit arrays

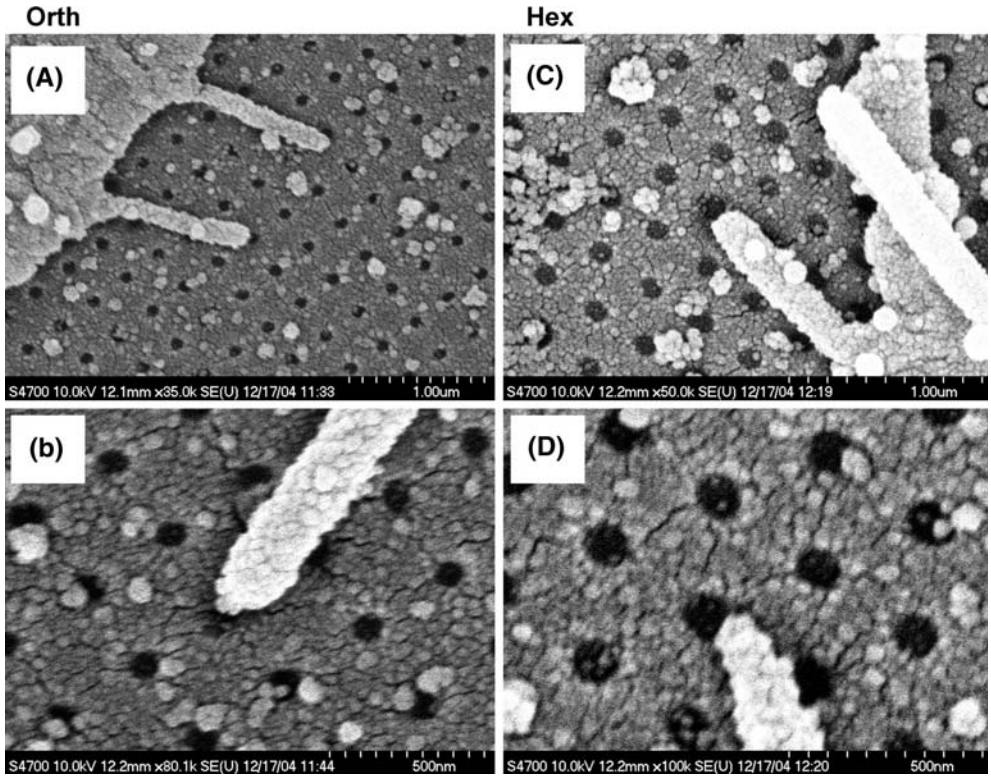

Fig. 4 High magnification scanning electron micrographs showing the size comparison of filopodial tips and the nanofeatures when cells were cultured on (**A**&**B**) square (sq) and (**C**&**D**) hexagonal (hex) topographies. Note the large number of interactions of filopodia with the lips of the pits

cultured on planar controls. It was seen that the significantly smaller cells produced the same numbers of filopodia than the much larger cells cultured on the planar surfaces. Thus, results were normalized by dividing the numbers of filopodia observed by perimeter measurements. It is important to note that the smaller perimeters are significantly different from control by $p < 0.05$, whereas the areas differ by $p < 0.01$. This is probably due to the increased stellation (invagination of the cell membranes for cells on the nanopits). Thus, it is shown that the normalisation is important as the cells growing on the topographies are far smaller than those on control.

Gustafson and Wolpert first described filopodia in living cells in 1961 [29]. Their study observed mesenchymal cells migrating up the interior wall of the blastocoelic cavity in sea urchins and noted that the filopodia produced appeared to explore the substrate, allowing them to speculate that they were being used to gather spatial information by the cells [30]. A wealth of literature builds a picture of filopodia as possibly being involved with both chemical and topographical sensing. In addition, filopodia have been associated with the detection of chemoattractent gradients [31, 32]. Whilst distinctly different from other cell filopodia, neuronal growth cone

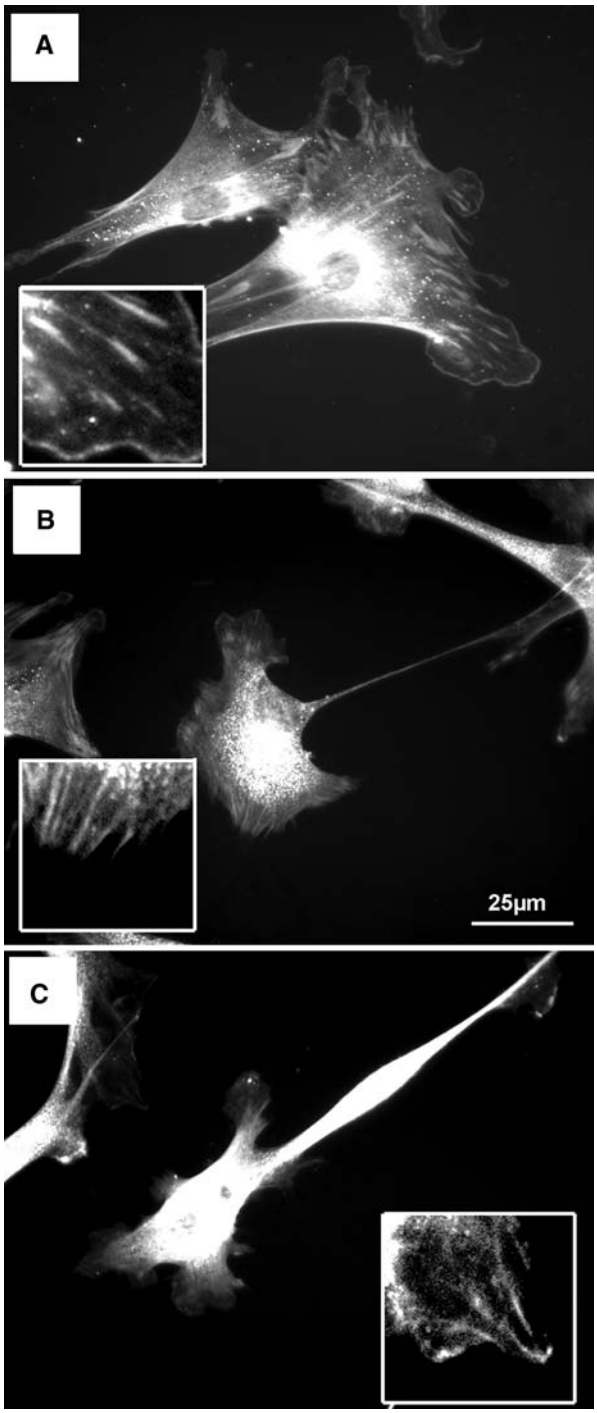

Fig. 5 Adhesion formation (vinculin stain) of osteoprogenitor cells on the test topographies. (**A**) Cells on the planar control could form large dash adhesions all around the cell perimeters. (**B**) Cells culture on the square (sq) topography had visible dash adhesions, but they were smaller and fewer in number. (**C**) Cells cultured on the hexagonal (hex) topography had very few adhesions

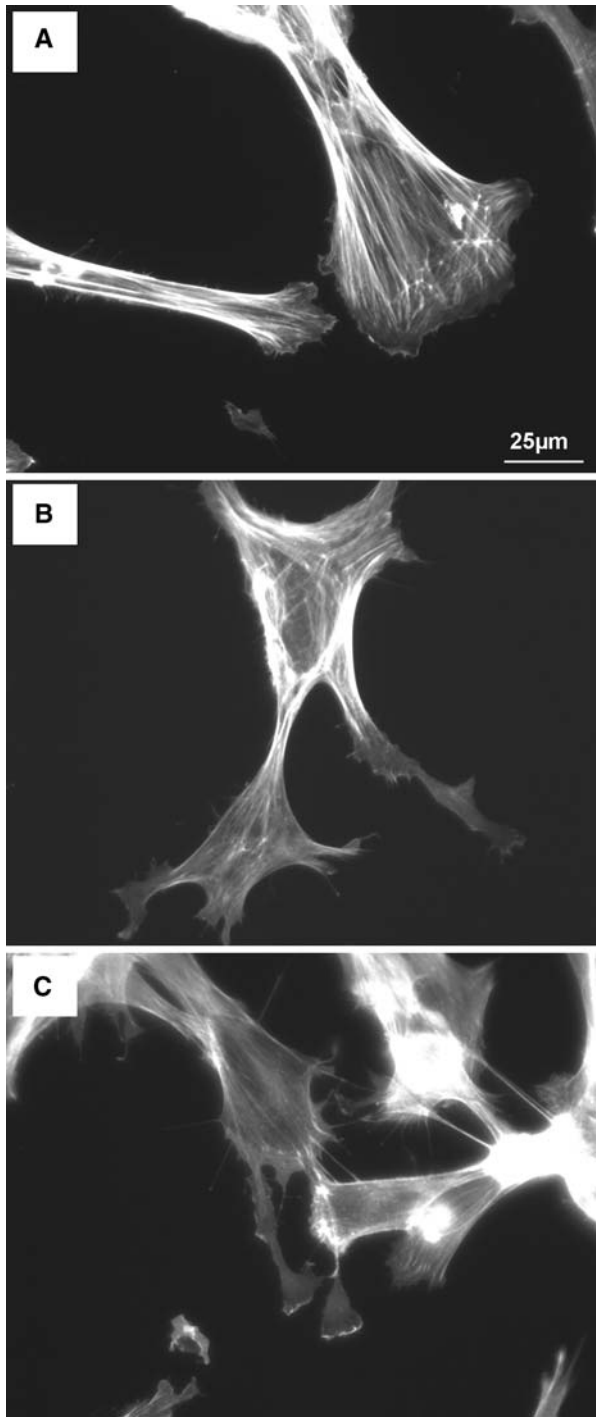

Fig. 6 Fluorescent actin staining in HMSC's on the test materials. (**A**) Cell with normal morphology and many actin stress fibres on flat control. (**B**) Stellate cell with many filopodia on square pits. (**C**) Stellate cells with many filopodia on hexagonal pits

filopodia have been described as sensing chemistry [33] and also as sensing microgrooves and then aligning neurons to the grooves [34–36].

Topography can also be used to change the morphology of cell filopodia. We have previously shown that by increasing the size of island topography from 13

to 35 to 95 nm, filopodia were observed to increase in thickness, until fibroblasts appeared almost amoeboid in shape [37]. The smallest structures filopodia have been observed to interact with were 10 nm high polymer demixed islands, again in fibroblasts [12]. Here, it was suggested that the filopodia were directing cell spreading, with adhesions forming in the filopodia as they 'sensed' a suitable area for attachment and then the cell lamellae being pulled over to the preferred sight. Fibroblast filopodia have also previously been studied reacting to 120 nm pits in an square arrangement, where a 54% incidence of filopodial/pit interaction was observed [13].

The generation of materials with islands of chemistry and topography provides insight into how cells sense and what materials features may provide cues to cells to elicit desirable growth patterns/reduced cell growth. It could be postulated such cues could be particularly important for undifferentiated, progenitor cells. In support of this theory is the increase from 54% incidence to 67% incidence of filopodial sensing from fibroblasts to HMSC's cultured on the square nanopits. This is remarkable when it is considered that the master substrates (in silicon) have a mere 12.6% surface coverage of pits (this increases to 27% when including the lips produced by embossing—note that these percentages represent the surface area of the material covered by pits from [13]).

In this study, it has been shown that, as with other cell types, these highly ordered nanopatterns have properties of low-adhesion and reduced cell spreading. Reduction in adhesion of tissue cell types may be of importance in the development of materials where biofouling can be problematic e.g. heart valve, femoral head/acetabular cup prosthesis, meshes for e.g. hernia repair, catherters, plates where tendon adhesion can be a troublesome.

We must note that whilst filopodia formation and subsequent adhesion maturation/lack of adhesion may be the cells first response to a material, it will be the initial protein/material interaction that will be critical. Highly organised nanoarrays, as used here, tend to produce hydrophobic surfaces (and can even form superhydrophobic surfaces if their aspect ratios are large enough) [38]. Hydrophobic surfaces are less wettable and thus tend to be low-adhesion due to lack of protein recruitment [8].

As shown by vinculin immunolocalisation, and as predicted from the above, the ability of the cells to form focal adhesions was reduced as was the ability of the cells to organise their actin cytoskeleton. Adhesion and cytoskeletal formation is critical in cell signalling. Adhesions are the cells link to the extracellular environment, with transmembrane integrin proteins within the adhesions linking to ligands in the extracellular matrix (e.g. RGD) and linking to internal adhesion proteins involved with action (e.g. vinculin). Changing the adhesive properties of a material will impact on many signalling pathways, hence affecting cell growth, proliferation and tissue formation.

5 Conclusion

The current study using human mesenchymal populations suggests a potential role for filopodia in spatial sensing and attachment. Again, the highly ordered nanopits, most notably the hex pattern, significantly reduced cell adhesion and spreading as shown by immunofluorescence and image analysis and thus have possible use in areas where reduced biofouling may be of advantage.

Acknowledgements MD is a BBSRC David Phillips Fellow (17/JF/20604) and is funded through this route. N. Gadegaard is a Royal Society of Edinburgh research fellow. ROCO is supported by grants from the BBSRC and EPSRC. We would like to thank John Pedersen (SDC Dandisc A/S, Denmark) for the organising and preparation of nickel shims and Stephanie Inglis for assistance with cell culture. We also thank Prof Adam Curtis and Dr Mathis Riehle for their support and discussion.

References

1. A. S. G. CURTIS and M. VARDE, *J. Natl. Cancer Res. Inst.* **33** (1964) 15.
2. S. BRITLAND, H. MORGAN, B. WOJCIAK-STOTHARD, M. RIEHLE, A. CURTIS and C. WILKINSON, *Exp. Cell Res.* **228** (1996) 313.
3. B. WOJCIAK-STOTHARD, A. CURTIS, W. MONAGHAN, K. MACDONALD and C. WILKINSON, *Exp. Cell. Res.* **223** (1996) 426.
4. B. WOJCIAK-STOTHARD, A. S. G. CURTIS, W. MONAGHAN, M. MCGRATH, I. SOMMER and C. D. W. WILKINSON, *Cell Motil. Cytoskeleton* **31** (1995) 147.
5. P. CLARK, P. CONNOLLY, A. S. CURTIS, J. A. DOW and C. D. WILKINSON, *Development* **99** (1987) 439.
6. P. CLARK, P. CONNOLLY, A. S. CURTIS, J. A. DOW and C. D. WILKINSON, *Development* **108** (1990) 635.
7. M. J. DALBY, M. O. RIEHLE, S. J. YARWOOD, C. D. WILKINSON and A. S. CURTIS, *Exp. Cell. Res.* **284** (2003) 274.
8. B. KASEMO and J. LAUSMAA, *Int. J. Oral Maxillofac. Implants* **3** (1988) 247.
9. B. KASEMO and J. LAUSMAA, *Environ. Health Perspect.* **102**(Suppl 5) (1994) 41.
10. A. D. BERSHADSKY, N. Q. BALABAN and B. GEIGER, *Annu. Rev. Cell Dev. Biol.* **19** (2003) 677.
11. K. BURRIDGE and M. CHRZANOWSKA-WODNICKA, *Annu. Rev. Cell Dev. Biol.* **12** (1996) 463.

12. M. J. DALBY, M. O. RIEHLE, H. JOHNSTONE, S. AFFROSSMAN and A. S. CURTIS, *Cell Biol. Int.* **28** (2004) 229.
13. M. J. DALBY, N. GADEGAARD, M. O. RIEHLE, C. D. WILKINSON and A. S. CURTIS, *Int. J. Biochem. Cell Biol.* **36** (2004) 2015.
14. J. HUANG, L. DI SILVIO, M. WANG, K. E. TANNER and W. BONFIELD, *J. Mater. Sci. Mater. Med.* **8** (1997) 775.
15. M. J. DALBY, L. DI SILVIO, E. J. HARPER and W. BONFIELD, *Biomaterials* **23** (2002) 569.
16. J. HUANG, L. DI SILVIO, M. WANG, I. REHMAN, C. OHTSUKI and W. BONFIELD, *J. Mater. Sci. Mater. Med.* **8** (1997) 809.
17. M. J. DALBY, D. PASQUI and S. AFFROSSMAN, *IEE Proc. Nanobiotechnol*. **151** (2004) 53.
18. M. J. DALBY, M. O. RIEHLE, D. S. SUTHERLAND, H. AGHELI and A. S. CURTIS, *Biomaterials* **25** (2004) 5415.
19. D. R. S. CUMMING, S. THOMS, S. P. BEAUMONT and J. M. R. WEAVER, *Appl. Phys. Lett.* **68** (1996) 322.
20. C. VIEU, F. CARCENAC, A. PEPIN, Y. CHEN, M. MEJIAS, A. LEBIB, L. MANIN-FERLAZZO, L. COURAUD and H. LAUNOIS, *Appl. Surf. Sci* **164** (2000) 111.
21. N. GADEGAARD, S. THOMS, D. S. MACINTYRE, K. MCGHEE, J. GALLAGHER, B. CASEY and C. D. W. WILKINSON, *Microelectron Eng* **67–68** (2003) 162.
22. N. GADEGAARD, S. MOSLER and N. B. LARSEN, *Macromol. Mater. Eng.* **88** (2003) 76.
23. H. SCHIFT, C. DAVID, M. GABRIEL, J. GOBRECHT, L. J. HEYDERMAN, W. KAISER, S. KOPPEL and L. SCANDELLA, *Microelectron. Eng.* **53** (2000) 1.
24. R. O. OREFFO, S. BORD and J. T. TRIFFITT, *Clin. Sci. (Lond)* **94** (1998) 549.
25. X. B. YANG, H. I. ROACH, N. M. P. CLARK, S. M. HOWDLE, R. QUIRK, K. M. SHAKESHEFF and R. O. C. OREFFO, *Bone* **29** (2001) 523.
26. A. S. CURTIS, B. CASEY, J. O. GALLAGHER, D. PASQUI, M. A. WOOD and C. D. WILKINSON, *Biophys. Chem.* **94** (2001) 275.
27. J. O. GALLAGHER, K. F. MCGHEE, C. D. W. WILKINSON and M. O. RIEHLE, *IEEE Trans. Nanobiosci.* **1** (2002) 24.
28. A. S. CURTIS, N. GADEGAARD, M. J. DALBY, M. O. RIEHLE, C. D. WILKINSON and G. AITCHISON, *IEEE Trans. Nanobiosci.* **3** (2004) 61.
29. T. GUSTAFSON and L. WOLPERT, *Exp. Cell Res.* **24** (1961) 64.
30. W. WOOD and P. MARTIN, *Int. J. Biochem. Cell Biol.* **34** (2002) 726.
31. M. UEDA, Y. SAKO, T. TANAKA, P. DEVREOTES and T. YANAGIDA, *Science* **294** (2001) 864.
32. M. IIJIMA and P. DEVREOTES, *Cell* **109** (2002) 599.
33. A. J. KOLESKE, *Sci. STKE* **2003** (2003) pe20.
34. A. RAJNICEK, S. BRITLAND and C. MCCAIG, *J. Cell. Sci.* **110**(Pt 23) (1997) 2905.
35. A. RAJNICEK and C. MCCAIG, *J. Cell. Sci.* **110**(Pt 23) (1997) 2915–2924.
36. E. STEPIEN, J. STANISZ and W. KOROHODA, *Cell. Biol. Int.* **23** (1999) 105.
37. M. J. DALBY, M. O. RIEHLE, H. J. JOHNSTONE, S. AFFROSSMAN and A. S. CURTIS, *Tissue Eng.* **8** (2002) 1099.
38. E. MARTINES, K. SEUNARINE, H. MORGAN, N. GADEGAARD, C. D. W. WILKINSON, M. O. RIEHLE, *Nanoletters* **5** (2005) 2097.